ASEAN Engineering Journal

Full Paper

HAND RECOGNITION SYSTEM BASED ON ELECTROMYOGRAPHY FOR REAL-TIME HAND PROSTHETIC CONTROL

Nida Sae Jong, Sakariya Sa-e, Ahmad Tirasor, Nifadila Mama, Hassan Dao*

Faculty of Engineering, Princess of Naradhiwas University, Narathiwat, 96000, Thailand

Article history
Received
19 May 2022
Received in revised form
11 September 2022
Accepted
03 October 2022
Published online
28 February 2023

*Corresponding author
hassan@pnu.ac.th

Graphical abstract

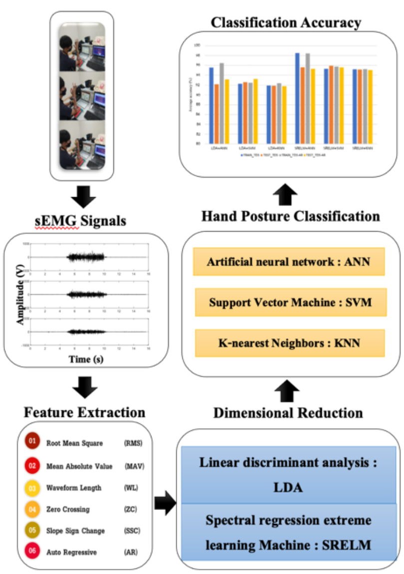

Abstract

Upper limb amputation is a significant limitation for achieving routine activities. Myoelectric signals detected by electrodes well-known as Electromyography (EMG) have been targeted to control upper limb prostheses of such lost limbs. Unfortunately, the acquisition, processing and use of such myoelectric signals are sophisticated. Furthermore, it necessarily requires complex computation to fulfil accuracy, robustness, and time-consumption execution for the real-time prosthesis application. Thus, machine learning schemes for pattern recognition are a potential approach to improve the traditional control for hand prostheses due to the movement of users and muscle contraction. This paper presents real-time hand posture recognition based on three hand postures using surface EMG (sEMG) signals. sEMG signals are acquired by the electrode channel and simultaneously collected while making a hand posture. Performance evaluation relies on classification accuracy and time consumption. The performance of six real-time recognition models is evaluated which combine two projection techniques and three classifiers. Results indicate that EMG-based pattern recognition (EMG-PR) control outperforms the traditional control for hand prostheses in real-time application. The highest classification accuracy is approximately 96%, whereas the lowest time consumption is 4 ms. In addition, the accuracy is dropped when the number of electrodes decreases nearly to 3%. These outcomes can apply to real-time hand prostheses to alleviate the limited prostheses available.

Keywords: Upper limb, Hand prosthesis, Hand Posture, Electromyography, Pattern recognition.

1.0 INTRODUCTION

The number of humans with loss of a limb tend to increase, which significantly affects their abilities to do daily activities. Therefore, the use of artificial prostheses is important for their well-being [1, 2]. In recent decade, the research of upper limb prosthesis control has been widely proposed. Different studies focused on improving robust prosthesis control in real time [3, 4]. Consequently, pattern recognition control systems have been developed extensively in academic research and have been seen in commercial production recently [3, 5, 6].

Currently, sEMG signals have been used to control the function of the prosthetic hand. sEMG signals are measurements of the action potential along motor neurons, which are extremely low-level signals. Generally, the amplitude of sEMG signal varies from 0 to 10 millivolts and the frequency range is between 20 and 450 Hz [3]. The hand prostheses control based sEMG signals can be divided into two types such as the proportional control and pattern recognition control. However, the proportional control has a limitation for controlling the motor speed, which depends on the threshold of the defined signals. Since the residual sEMG signals have fluctuated, pattern recognition control based on sEMG signals has been developed to increase the performance of the prosthetic hands [3, 5].

Some challenges in pattern recognition research are the large number of electrodes, system complexity, and the real time processing that provide the high performance for hand prostheses [1, 3, 5]. Therefore, the classification accuracy, the processing time, and the user friendly shall be considered.

Hameed et al. proposed the muscle locations on the upper limb used for rehabilitation robot of stroke patients. Flexor digitorum and extensor digitorum were commonly operated to control robotic gloves [7]. Normally, the pattern recognition consists of filtering, segmentation data, feature extraction, dimensional reduction, and classification. Parajuli et al. presented the existing pattern recognition methods used in prosthetic hand control based on sEMG signals [3]. The results showed that there were manifold methods of recognizing hand postures conform to the previous pattern recognition process. For instance, different classifiers were applied to evaluate the system performance including linear, learning, and statistical algorithms [1].

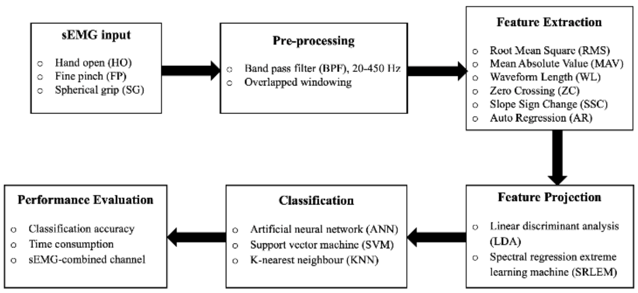

Figure 1 Flow diagram of hand posture recognition processing.

The overview of the hand posture recognition diagram is shown in Figure 1. The sEMG signals are primarily measured and collected when the volunteers stretch and contract the muscles for three hand postures. Then, the pre-processing process including filtering and windowing techniques is applied for cleaning inherent disturbances and feeding to the feature extraction process, respectively. Two feature groups including six-time domain features are subsequently calculated to decrease the signal sophistication. Henceforth, two distinct projection algorithms are used to lower the dimension of the retrieved data. Finally, three classifiers are obtained to categorize the hand postures.

Data acquisition and processing method of sEMG signals based on three hand postures are discussed in Section 2. The results are discussed and presented in Section 3. Section 4 concludes and provides an overall analysis of the paper.

2.0 METHODOLOGY

This section presents data acquisition and processing method. The data acquisition demonstrates attainable approach to obtain the sEMG signals while the proposed method describes the recognition processing for hand postures.

2.1 Data Acquisition

The EMG signals of forearm muscles were initially collected by five healthy volunteers between 20 and 22 years of ages (two women and three men). In this experiment, sEMG signals were acquired by electrodes distributed into three channels, namely Flexor digitorum (CH1), Extensor digitorum (CH1), and Extensor pollicis longus (CH1) [8] as shown in Figure 2. The characteristic of each channel was designed in a bipolar plate and the ground electrode (green one) was put on the right wrist.

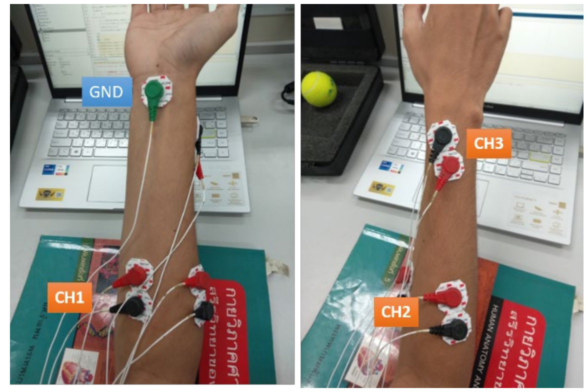

Figure 2 Electrode placement of 3-channel sEMG and ground electrode.

While the sEMG signals from CH2, CH3, CH4, and CH5 were recorded with the monopolar configuration, the sEMG signals from CH1 were recorded with the bipolar configuration. The reference electrode was placed on the earlobe and the ground electrode was placed on the left wrist. Small disc-shaped sEMG electrodes (5 mm diameter, Ag/AgCl) and shielded cables were connected to a commercial sEMG measurement system for recording sEMG signals. The sEMG signals were digitized at a sampling frequency of 1024 Hz.

Table 1 Computer specification for processing

Component	Specification
Processor	AMD Ryzen 7 4800H (2.90 GHz, 4MB L2 cache)
Memory	24 GB DDR4, 4266 MHz
Hard drive	1 TB SSD
Graphics	Radeon Graphics 448SP
Operating System	Windows 11, 64 bit

The sEMG signals were measured using the commercial equipment (TMSi) through cables and a small disc-shaped sEMG electrodes (52 mm diameter, Ag/AgCl). The data were subsequently sent to the computer via Bluetooth and were collected using Porti. The computer specification is shown in Table 1.

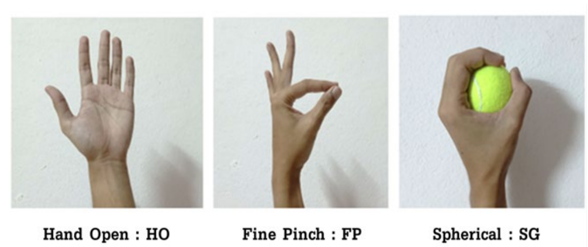

Figure 3 Three grasps comprise of hand open, fine pinch and spherical grip.

Every volunteer was requested to conduct the three grasps composed of hand open (HO), fine pinch (FP), and spherical grip (SG) [9, 10, 11, 12, 13] as shown in Figure 3. Each grasp was repeated 10 times for five seconds to test the robustness of the classifier. There are 10 seconds of rest for each pose. Thus, each volunteer managed to produce of 90 samples of sEMG signals (3 grasps x 3 channels x 10 trials). Figure 4 illustrates a case in point of the measured sEMG signals from the Hand open.

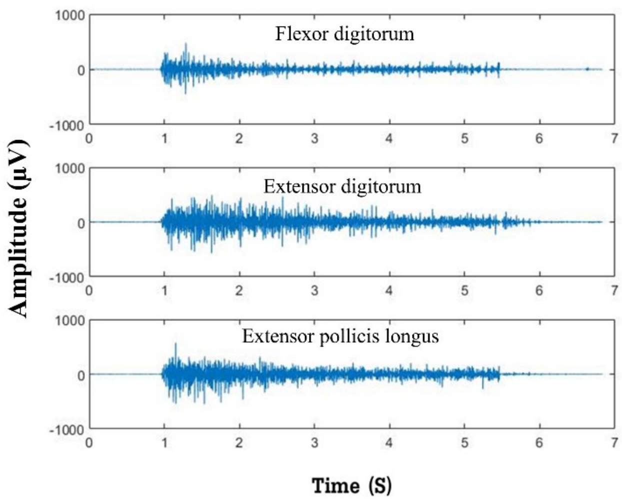

Figure 4 Example of the 3-channel sEMG signal based on the Hand open.

2.2 Data Processing

The proposed pattern recognition diagram for hand prostheses is shown in Figure 5. The feature vector length is denoted by a number in parenthesis. The feature calculation step generates feature vectors from two feature groups, whose lengths are 15 and 27, respectively. The min-max normalization method was used to norm data in the same range.

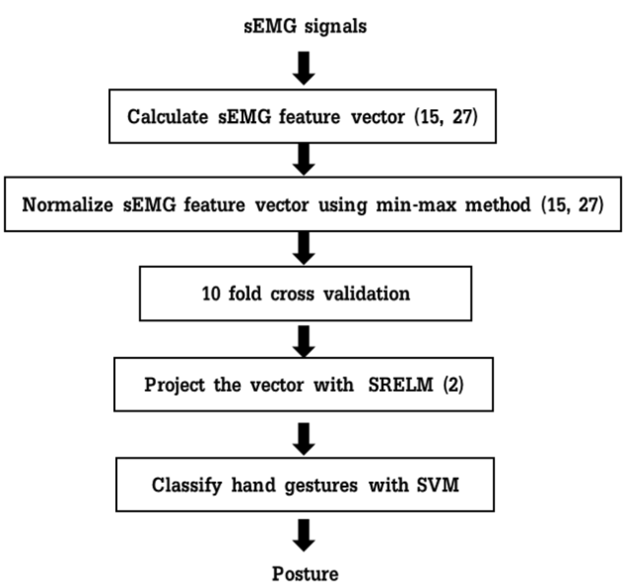

Figure 5 Proposed pattern recognition block diagram for hand prostheses.

The normalized data are divided into 10 subsets called 10-fold cross validation to test the performance of model. Then, the feature projection can reduce the lengths of normalized feature vectors from both feature groups to 2. The classification of the hand postures relies on three algorithms.

2.2.1 Pre-Processing

The motion artifact and different noise sources of the bandwidth sEMG signals are removed by applying a bandpass filter with suitable cutoff frequencies of 20-450 Hz. An example of raw signal for fine pinch posture and filtered signal is presented in Figure 6. Secondly, 5120 sample length of the sEMG signal is segmented to posture time interval of 5 s. Finally, the features are evaluated using an adjacent windowing technique with 150 ms window length and 50ms overlapping to refrain from unacceptable delays in real-time operations [14, 15]

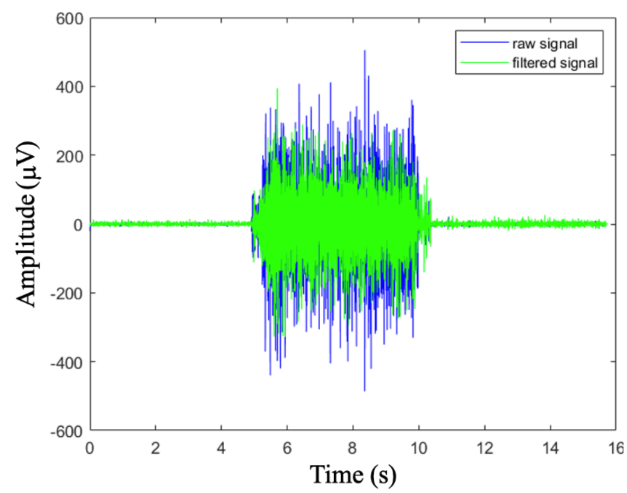

Figure 6 The raw signal and filtered signal of fine pinch.

2.2.2 Feature Extraction

Generally, the time domain feature shows the best result based on pattern recognition for hand prostheses [3, 16]. The various time-domain features using in real time pattern recognition for hand prostheses are proposed, especially Mean Absolute Value (MAV), Waveform Length (WL), Zero Crossing (ZC), and Slope Sign Change (SSC). These features are investigated and evaluated for achieving the high classification accuracy. Moreover, adding Auto regressive (AR) features can employ higher classification efficiency for hand movements detection based on sEMG signals. Lui and Huang [17] recommend that a fourth-order autoregressive model can improve the performance. The sEMG features are divided into two groups, such as five-time domain feature, TD5 (MAV, RMS, WL, ZC, SSC) and TD5 with forth-order autoregressive, TD5-4AR in this research. Details of feature extraction are described as follows.

MAV: assigns the sEMG signal amplitude in a sampled segment which can be defined as [18]

$$MAV = \sum_{i=1}^{N} |x_i| \tag{1}$$

Where, x_i is the amplitude of sEMG signal at sample i, N denotes the total number of sEMG samples

RMS: defines the magnitude of sEMG signal alike MAV as shown in (2) [6]

$$RMS = \sqrt{\frac{1}{N}\left(\sum_{i=1}^{N} x_i^2\right)} \tag{2}$$

WL: defines how intricate sEMG signal which characterizes the samples of sEMG waveform cumulative length [18]. The WL can be expressed as,

$$WL = \sum_{i=1}^{N-1} |x_{i+1} - x_i| \tag{3}$$

ZC: defines the frequency information of the sEMG signal measurement and indicates how many times the sEMG signal's amplitude value crosses the zero-amplitude level. A threshold, T is executed to abstain low voltage fluctuations or background noises [18].

$$ZC = \sum_{i=1}^{N} [f(x_i \times x_{i+1}) \text{ and } |x_i - x_{i+1}| \geq T] \tag{4}$$

Where, $f(x) = \begin{cases} 1, & x < 0 \\ 0, & x > 0 \end{cases}$

SSC: is an additional element of the signal frequency defined by

$$\sum_{i=2}^{N-1} [s\{(x_i - x_{i-1})(x_i - x_{i+1})\}] \tag{5}$$

Where, $s(x) = \begin{cases} 1, & x < 0 \\ 0, & x > 0 \end{cases}$

AR: uses a linear combination of the prior observation value x_{i-p} and white noise w_p, to estimate the presented value defined by [18].

$$AR = \sum_{p=0}^{p-1} a_p x_{i-p} + w_p \tag{6}$$

Where, *P* is the order of the AR model, 4th order AR and coefficient of 4 were applied in this experiment.

sEMG features are extricated and concatenated from all channels and subsequently the data is normalized by the min-max normalization techniques. The results consequently have a range of -1 to 1. The normalized data dimension for both feature groups are 3000 rows, with 15 columns and 27 columns for features TD5 and TD5-4AR, respectively.

2.2.3 Feature Projection

Feature projection is one of the dimensional reduction techniques to reduce the computation cost and increase the information relevance. Several projection algorithms apply to pattern recognition control of hand prostheses such as principal component analysis (PCA), linear discriminant analysis (LDA) and spectral regression extreme learning machine (SRELM). LDA is commonly used in real time pattern recognition control because the results perform high accuracy and low complexity computation. Moreover, the SRELM method provides the high performance for pattern recognition in recent studies [19, 20]. Therefore, two projection techniques were applied in this research to compare the classification accuracy and time consumption. In short, SRELM combines extreme learning machine (ELM) and spectral regression (SR), with the generated eigenvector being used to project the output layer [19]. The hidden layer weights are random determined, whereas SR calculates the output weight using the least squares approach to determine the optimum projection direction. The quantity of concealed nodes and alpha [19] are two parameters that can be tweaked to improve SRELM performance. To find the best parameters, the number of concealed nodes is fluctuated between 100 and 1,500 with 100 node increase, whereas the variation of alpha is obtained between 1 and 20 with 1 increment.

The normalized data is divided into two parts including training and testing data and the ratio of training and testing data is 80 to 20, respectively. Next, the 10-fold cross validation will divide the training data into 10 subsets, with nine subsets used for learning and another subset used for classifier testing [21]. This process is implemented 10 times, which each subset serving as the testing data. Then, both LDA and SRELM are employed to reduce the dimension of learning data from 3000 rows × 15 columns (TD5) and 3000 rows × 27 columns (TD5-AR) to 3000 rows × 2 columns.

2.2.4 Classification

The projected features are classified to three hand postures using three algorithms including feedforward neural network of Artificial neural network (ANN), support vector machine (SVM) and k-nearest neighbour (KNN). A feed forward neural network comes with a structure which is composed of an input layer, a hidden layer, and an output layer. The length of the projected vector is 2 to determine the number of nodes in the input layer. Finding the best number in the hidden layer, the numbers of nodes in the hidden layer are varied from 15 to 25. Node number of 20 is find the best accuracy in this hidden layer. The output layer has three nodes, which corresponds to the number of hand postures. A hyperbolic tangent sigmoid is used as the transfer function for the hidden and output layers. A coarse grid-search strategy is used to find the best SVM parameters. SVM is employed in conjunction with the radial basis function kernel. The cost parameter C's and kernel parameter's parameter ranges are as γ are between 10^{-3} - 10^{3}**.** For KNN, the Euclidean distance is used to evaluate the similarity between new data and available categories by varying the number of k which are 3, 5, and 7 respectively.

3.0 RESULTS AND DISCUSSION

The results are divided into three parts. The first part is classification accuracy which suggests the effective comparison among various models. The second part is time consumption that represents the computed time in testing process. The final section provides a comparison of the performance of sEMG-combined channels into two to three channels.

3.1 Classification Accuracy

The system performance of six models, namely LDA-ANN, LDA-SVM, LDA-KNN, SRELM-ANN, SRELM-SVM and SRELM-KNN have been compared. The average classification accuracy and standard deviation (SD) for three hand postures obtained by 3 sEMG-combined channels from five subjects are shown by Figure 7 and Table 2 respectively. For instance, LDA-ANN indicates the combination of LDA for dimensional reduction and ANN for classification. There are four bar graphs in each model that presents the accuracy of train and test data of two feature groups, TD5 and D5-AR. SRELM-SVM evidently shows the highest classification accuracy in testing, especially TD5 is approximately up to 96%. The efficacy of SRELM-ANN is close to SRELM-SVM of both feature groups although there is broad variation of training and testing accuracies. This result is not applicable for hand gesture recognition which may be affected by the over-fitting between the training and testing data.

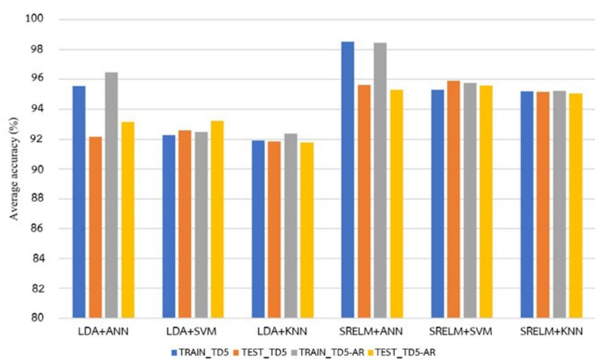

Figure 7 Average accuracy of six algorithms from five subjects of three hand postures.

Table 2 Accuracy with standard deviation of different algorithms

Algorithms	Accuracy with standard deviation	
	TD5	TD5-AR
LDA-ANN	92.2 ± 0.3	93.1 ± 0.3
LDA-SVM	92.6 ± 0.2	93.2 ± 0.2
LDA-KNN	91.9 ± 0.6	91.8 ± 0.5
SRELM-ANN	95.6 ± 0.3	95.3 ± 0.3
SRELM-SVM	95.9 ± 0.2	95.6 ± 0.2
SRELM-KNN	95.2 ± 0.3	95.1 ± 0.4

To attain a comprehensive insight of classification accuracy, Figure 8 shows scatterplot between the first two elements of the project vectors from 3 hand postures. Project feature vectors from LDA-ANN, LDA-SVM, and LDA-KNN in Figure 5(a)-5(c) respectively are slightly overlapped, corresponding to the average accuracy at 92%. SRELM-ANN, SRELM-SVM, and SRELM-KNN in Figure 5(d) - 5(f) are discernable degree of separation, corresponding to average accuracy up to 96%.

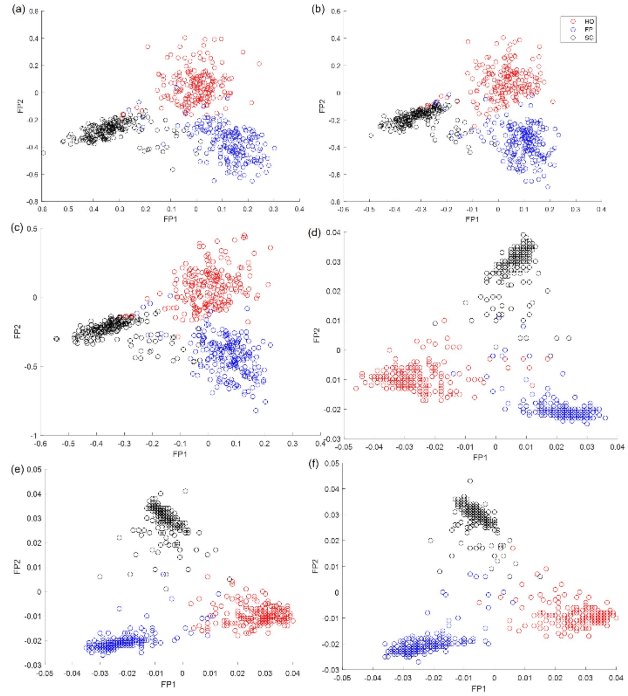

Figure 8 Scatter plots of the projected feature vector of TD5 : (a) LDA-ANN, (b) LDA-SVM, (c) LDA-KNN, (d) SRELM-ANN, (e) SRELM-SVM, and (f) SRELM-KNN

In additional, LDA-KNN provides the lowest classification accuracy of nearly 92%. Considering the capability of feature projection, classification accuracy of SRELM is explicitly higher than LDA for all classifiers. In view of feature groups, the result shows that there is no significant distinctness. Some algorithms indicate that the efficacy of TD5 is higher than TD5-AR including LDA-KNN, SRELM-ANN, SRELM-SVM and SRELM-KNN, while the other algorithms are not identical performing. For the comparison of the three classifiers, the performance of ANN is comparable to SVM whereas KNN provides the lowest capability. However, KNN implies stabler since the accuracy of training and testing data is resemblant.

3.2 Time Consumption

Figure 9 shows comparison of time consumption in testing process of the six models. The time consumption obtains less than 12 ms except SRELM-ANN. Moreover, LDA-KNN gives the shortest time required for testing data at approximately 4 ms for both TD5 and TD5-AR. In contrast, SRELM-ANN gives the highest testing time especially in TD5-AR about 27 ms. However, considering the recognition performance, SRELM-SVM with TD5 is the optimal model that presented the highest classification accuracy of nearly 96% and low time consumption of approximately 10 ms.

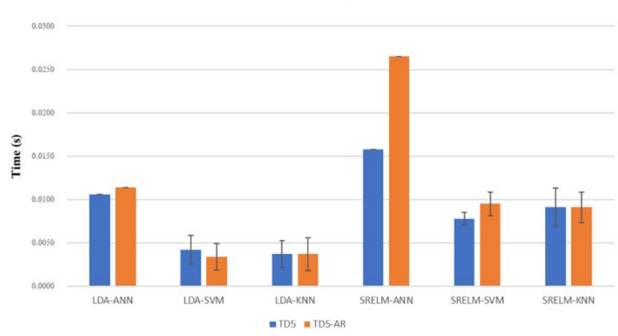

Figure 9 Time consumption in testing process of the six models.

3.3 Performance Evaluation

From the preceding outcomes, SRELM-SVM has potential opportunity to commerce and is thus selected to evaluate the efficiency of 2 sEMG-combined channels. Figure 10 presents the average accuracy of the channels based on SRELM-SVM. Horizonal axis represents the electrode channels, for instance, CH1-2 indicates the data channel 1 and 2. The overall accuracy of five patients improves from 90% to 96 % by adding quantity of CH2-3 sEMG-combined channels. Based on the results, CH1 and CH3 are the best two sEMG-combined channels with a maximum accuracy of 93 %. On the other hand, with the added quantity of sEMG-combined signals from two to three, the average accuracy values move up about 3% to 6% depending on the electrode position.

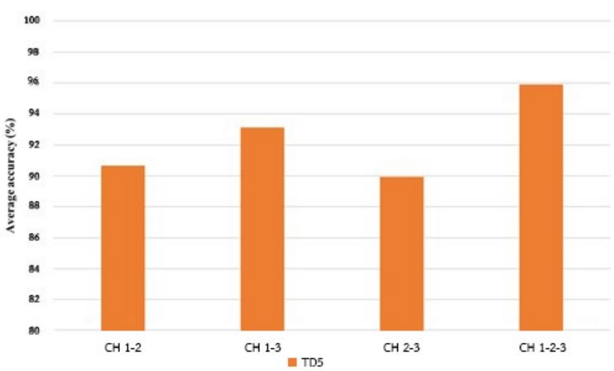

Figure 10 Comparison of two and three channel accuracies.

4.0 CONCLUSION

This paper presents a recognition classification using sEMG signals for controlling hand prostheses based on three hand postures. The real-time hand recognition models are also evaluated. The six models which represent the combination of dimensional reduction and classification methods are employed to recognize the hand postures from three channels of sEMG signals.

The results significantly express that SRELM-SVM model is satisfactory to apply in real-time pattern recognition control. It outperforms other models for both classification accuracy and time consumption. Furthermore, the classification accuracy of 2 sEMG-combined channels is comparable to all channel accuracy. Hence, the data obtained from the study can be used as a reference and development of a pattern recognition control for prosthetic hand of impaired patients.

Acknowledgement

We gratefully thank the Faculty of Engineering, Princess of Naradhiwas University for financial support.

References

[1] Igual, C., Pardo, L. A., Hahne, J. M., Igual, J., 2019 "Myoelectric control for upper limb prostheses," . *Electronics*. 8(11): 1244 doi: 10.3390/electronics8111244.

[2] Geethanjali, P., 2016. "Myoelectric control of prosthetic hands: State-of-the-art review," *Medical Devices: Evidence and Research*. doi: 10.2147/MDER.S91102.

[3] Parajuli, N., Sreenivasan, N., Bifulco, P., Cesarelli, M., Savino, S., Niola, V., Esposito, D., Hamilton, T. J., Naik, G. R., Gunawardana, U., Gargiulo, G. D., 2019 "Real-time EMG based pattern recognition control for hand prostheses: A review on existing methods, challenges and future implementation," *Sensors (Switzerland)*. 19(20): 4596. doi: 10.3390/s19204596.

[4] Sattar, N. Y., Syed, U. A., Muhammad, S., Kausar, Z., 2019 "Real-time EMG signal processing with implementation of PID control for upper-limb prosthesis,". *International Conference on Advanced Intelligent Mechatronics (AIM) :120-125* doi: 10.1109/AIM.2019.8868796.

[5] Krasoulis, A., Kyranou, I., Erden, M. S., Nazarpour, K., Vijayakumar, S., 2017, "Improved prosthetic hand control with concurrent use of myoelectric and inertial measurements," *Journal of Neuro Engineering and Rehabilitation. 14(71): 1-14* doi: 10.1186/s12984-017-0284-4.

[6] Pradhan, A., He, J., Jiang, N., 2021, "Performance Optimization of Surface Electromyography Based Biometric Sensing System for Both Verification and Identification," *IEEE Sensors Journal.* 21(19): 21718-21729. doi: 10.1109/JSEN.2021.3079428.

[7] Hameed, H. K., Hassan, W. Z. W., Shafie, S., Ahmad, S. A., Jaafar, H., 2020. "A Review on Surface Electromyography-Controlled Hand Robotic Devices Used for Rehabilitation and Assistance in Activities of Daily Living," *Journal of Prosthetics and Orthotics*. 32(1): 3-13 doi: 10.1097/JPO.0000000000000277.

[8] Li, G., 2011. "Electromyography Pattern-Recognition-Based Control of Powered Multifunctional Upper-Limb Prostheses," in *Advances in Applied Electromyography*, 6. London, United Kingdom. doi: 10.5772/22876.

[9] Li, W., Shi, P., Yu, H., 2021. "Gesture Recognition Using Surface Electromyography and Deep Learning for Prostheses Hand: State-of-the-Art, Challenges, and Future," *Frontiers in Neuroscience*. 15: *621885*. doi: 10.3389/fnins.2021.621885.

[10] Prakash, A., Sharma, S., 2021, "Single-channel surface electromyography (sEMG) based control of a multi-functional prosthetic hand," *Instrumentation Science & Technology*. 49(4): 428-444 doi: 10.1080/10739149.2021.1880933.

[11] Mohammadi, A., Lavranos, J., Choong, P., Oetomo, D., 2019. "X-limb: A soft prosthetic hand with user-friendly interface," in *Biosystems and Biorobotics*, 21: 82-86. doi: 10.1007/978-3-030-01845-0_16.

[12] Llop-Harillo, I., Pérez-González, A., Starke, J., Asfour, T., 2019, "The Anthropomorphic Hand Assessment Protocol (AHAP)," *Robotic and Autonomous Systems. 121: 103259*, doi: 10.1016/j.robot.2019.103259.

[13] Abbasi, B., Noohi, E., Parastegari, S., Zefran, M., 2016. "Grasp taxonomy based on force distribution," *2016 25th IEEE International Symposium on Robot and Human Interactive Communication (RO-MAN)*, New York, NY, USA, pp. 1098-1103. doi: 10.1109/ROMAN.2016.7745245.

[14] Nielsen, J. L. G., Holmgaard, S., Jiang, N., Englehart, K. B., Farina, D., Parker, P. A., 2011, "Simultaneous and proportional force estimation for multifunction myoelectric prostheses using mirrored bilateral training," *IEEE Transactions on Biomedical Engineering*, 58(3): 681-

688, doi: 10.1109/TBME.2010.2068298.

[15] Farrell, T. R., Weir, R. F., 2007, "The optimal controller delay for myoelectric prostheses," *IEEE Transactions on Neural Systems and Rehabilitation Engineering, 15(1): 111-118*, doi: 10.1109/TNSRE.2007.891391.

[16] Zhang, W., Shuai, L., Kan, H., 2021. "Real-time Gesture Recognition Based on Improved Artificial Neural Network and sEMG Signals," *2021 IEEE International Conference on Mechatronics and Automation (ICMA)*, Takamatsu, Japan, 981-986. doi: 10.1109/ICMA52036.2021.9512756.

[17] Liu, Y. H., Huang, H. P., 2009. "Towards a high-stability EMG recognition system for prosthesis control: A one-class classification based non-target EMG pattern filtering scheme," *2009 IEEE International Conference on Systems, Man and Cybernetics*, San Antonio, TX, USA, 4752-4757, doi: 10.1109/ICSMC.2009.5346086.

[18] Sae Jong, N., Phukpattaranont, P., 2019, "A speech recognition system based on electromyography for the rehabilitation of dysarthric patients: A Thai syllable study," *Biocybernetics and Biomedical Engineering, 39(1): 234-245* doi: 10.1016/j.bbe.2018.11.010.

[19] Anam, K., Al-Jumaily, A., 2015. "A novel extreme learning machine for dimensionality reduction on finger movement classification using sEMG," *2015 7th International IEEE/EMBS Conference on Neural Engineering (NER)*, Montpellier, France, 824-827, doi: 10.1109/NER.2015.7146750.

[20] Li, M., Wibowo, S., Li, W., Li, L. D., 2021, "Quantitative spectral data analysis u18sing extreme learning machines algorithm incorporated with pca," *Algorithms*, 14(1):. doi: 10.3390/a14010018.

[21] Jong, N. S., De Herrera, A. G. S., Phukpattaranont, P., 2021, "Multimodal Data Fusion of Electromyography and Acoustic Signals for Thai Syllable Recognition," *IEEE Journal of Biomedical and Health Informatics, 25(6): 1997-2006* doi: 10.1109/JBHI.2020.3034158.